# Second-order rogue wave breathers in the nonlinear Schrödinger equation with quadratic potential modulated by a spatially-varying diffraction coefficient

**Wei-Ping Zhong,[1,2,*] Milivoj Belić,[2] and Yiqi Zhang[3]**

[1]*Department of Electronic and Information Engineering, Shunde Polytechnic, Shunde 528300, China*
[2]*Texas A&M University at Qatar, P.O. Box 23874 Doha, Qatar*
[3]*Key Laboratory for Physical Electronics and Devices of the Ministry of Education & Shaanxi Key Lab of Information Photonic Technique, Xi'an Jiaotong University, Xi'an 710049, China*
**zhongwp6@126.com*

**Abstract:** Nonlinear Schrödinger equation with simple quadratic potential modulated by a spatially-varying diffraction coefficient is investigated theoretically. Second-order rogue wave breather solutions of the model are constructed by using the similarity transformation. A modal quantum number is introduced, useful for classifying and controlling the solutions. From the solutions obtained, the behavior of second order Kuznetsov-Ma breathers (KMBs), Akhmediev breathers (ABs), and Peregrine solitons is analyzed in particular, by selecting different modulation frequencies and quantum modal parameter. We show how to generate interesting second order breathers and related hybrid rogue waves. The emergence of true rogue waves – single giant waves that are generated in the interaction of KMBs, ABs, and Peregrine solitons – is explicitly displayed in our analytical solutions.



**OCIS codes:** (190.4420) Nonlinear optics, transverse effects; (190.3270) Kerr effect.

## References and links

1. B. A. Balomed, Nonlinear Schrödinger equations, in: *Encyclopedia of Nonlinear Science*, ed. by A. Scott (Routledge, 2005).
2. R. Höhmann, U. Kuhl, H. J. Stöckmann, L. Kaplan, and E. J. Heller, "Freak Waves in the Linear Regime: A Microwave Study," Phys. Rev. Lett. **104**(9), 093901 (2010).
3. Y. S. Kivshar and G. Agrawal, *Optical solitons: from fibers to photonic crystals* (Academic, 2003).
4. Y. Zhang, M. R. Belić, Z. Wu, H. Zheng, K. Lu, Y. Li, and Y. P. Zhang, "Soliton pair generation in the interactions of Airy and nonlinear accelerating beams," Opt. Lett. **38**(22), 4585–4588 (2013).
5. C. Kharif, E. Pelinovsky, and A. Slunyaev, *Rogue waves in the ocean* (Springer, 2009).
6. A. R. Osborne, Nonlinear Ocean Waves (Academic Press, 2009).
7. C. J. Pethick and H. Smith, *Bose–Einstein Condensation in Dilute Gases* (Cambridge University Press, 2002)
8. N. Akhmediev, A. Ankiewicz, and M. Taki, "Waves that appear from nowhere and disappear without a trace," Phys. Lett. A **373**(6), 675–678 (2009).
9. N. Akhmediev, J. M. Soto-Crespo, and A. Ankiewicz, "How to excite a rogue wave," Phys. Rev. A **80**(4), 043818 (2009).
10. E. A. Kuznetsov, "Solitons in a parametrically unstable plasma," Dokl. Akad. Nauk SSSR **236**, 575–577 (1977).
11. Y. C. Ma, "The perturbed plane-wave solution of the cubic Schrödinger equation," Stud. Appl. Math. **60**, 43–58 (1979).
12. N. Akhmediev and V. I. Korneev, "Modulation instability and periodic solutions of the nonlinear Schrodinger equation," Theor. Math. Phys. **69**(2), 1089–1093 (1986).
13. D. H. Peregrine, "Water waves, nonlinear Schrödinger equations and their solutions," J. Aust. Math. Soc. Ser. B **25**, 16–43 (1983).
14. A. N. Ganshin, V. B. Efimov, G. V. Kolmakov, L. P. Mezhov-Deglin, and P. V. E. McClintock, "Observation of an Inverse Energy Cascade in Developed Acoustic Turbulence in Superfluid Helium," Phys. Rev. Lett. **101**(6), 065303 (2008).
15. J. M. Dudley, G. Genty, and B. J. Eggleton, "Harnessing and control of optical rogue waves in supercontinuum generation," Opt. Express **16**(6), 3644–3651 (2008).

#231582 - $15.00 USD Received 29 Dec 2014; revised 24 Jan 2015; accepted 26 Jan 2015; published 5 Feb 2015

16. A. Montina, U. Bortolozzo, S. Residori, and F. T. Arecchi, "Non-Gaussian Statistics and Extreme Waves in a Nonlinear Optical Cavity," Phys. Rev. Lett. **103**(17), 173901 (2009).
17. Yu. V. Bludov, V. V. Konotop, and N. Akhmediev, "Matter rogue waves," Phys. Rev. A **80**(3), 033610 (2009).
18. Y. Zhang, M. R. Belić, H. B. Zheng, H. X. Chen, C. B. Li, J. P. Song, and Y. P. Zhang, "Nonlinear Talbot effect of rogue waves," Phys. Rev. E Stat. Nonlin. Soft Matter Phys. **89**(3), 032902 (2014).
19. J. M. Dudley, F. Dias, M. Erkintalo, and G. Genty, "Instabilities, breathers and rogue waves in optics," Nat. Photonics **8**(10), 755–764 (2014).
20. M. Onorato, S. Residori, U. Bortolozzo, A. Montina, and F. T. Arecchi, "Rogue waves and their generating mechanisms in different physical contexts," Phys. Rep. **528**(2), 47–89 (2013).
21. N. Akhmediev, J. M. Dudley, D. R. Solli, and S. K. Turitsyn, "Recent progress in investigating optical rogue waves," J. Opt. **15**(6), 060201 (2013).
22. W. P. Zhong, M. R. Belić, and T. Huang, "Rogue wave solutions to the generalized nonlinear Schrödinger equation with variable coefficients," Phys. Rev. E Stat. Nonlin. Soft Matter Phys. **87**(6), 065201 (2013).
23. W. P. Zhong, "Rogue wave solutions of the generalized one-dimensional Gross-Pitaevskii equation," J. Nonlinear Opt. Phys. Mater. **21**(2), 1250026 (2012).
24. C. N. Kumar, R. Gupta, A. Goyal, S. Loomba, T. S. Raju, and P. K. Panigrahi, "Controlled giant rogue waves in nonlinear fiber optics," Phys. Rev. A **86**(2), 025802 (2012).
25. C. Q. Dai, G. Q. Zhou, and J. F. Zhang, "Controllable optical rogue waves in the femtosecond regime," Phys. Rev. E Stat. Nonlin. Soft Matter Phys. **85**(1), 016603 (2012).
26. C. Q. Dai and W. H. Huang, "Controllable mechanism of breathers in the (2+1)-dimensional nonlinear Schrödinger equation with different forms of distributed transverse diffraction," Phys. Lett. A **378**(16), 1113–1118 (2014).
27. K. Manikandan, P. Muruganandam, M. Senthilvelan, and M. Lakshmanan, "Manipulating matter rogue waves and breathers in Bose-Einstein condensates," Phys. Rev. E Stat. Nonlin. Soft Matter Phys. **90**(6), 062905 (2014).
28. J. S. He, Y. S. Tao, K. Porsezian, and A. S. Fokas, "Rogue wave management in an inhomogeneous Nonlinear Fibre with higher order effects," J. Nonlin. Math. Phys. **20**(3), 407–419 (2013).
29. S. Loomba, R. Gupta, H. Kaur, and M. S. Mani Rajan, "Self-similar rogue waves in an inhomogeneous generalized nonlinear Schrödinger equation," Phys. Lett. A **378**(30), 2137–2141 (2014).
30. W. P. Zhong, L. Chen, M. Belić, and N. Petrović, "Controllable parabolic-cylinder optical rogue wave," Phys. Rev. E Stat. Nonlin. Soft Matter Phys. **90**(4), 043201 (2014).
31. D. J. Kedziora, A. Ankiewicz, and N. Akhmediev, "Second-order nonlinear Schrödinger equation breather solutions in the degenerate and rogue wave limits," Phys. Rev. E Stat. Nonlin. Soft Matter Phys. **85**(6), 066601 (2012).
32. N. Akhmediev and J. M. Dudley, "N-modulation signals in a single mode optical waveguide under nonlinear conditions," Sov. Phys. JETP **67**(1), 89–95 (1988).
33. V. B. Matveev and M. Salle, *Darboux Transformations and Solitons* (Springer-Verlag, 1991).

## 1. Introduction

Nonlinear Schrödinger (NLS) equation is a general model used to describe evolution of slowly-varying wave packets in various nonlinear systems [1,2]. It arises in many areas of nonlinear science, including optical beam propagation in nonlinear media [3,4], surface waves in deep ocean [5,6], and Bose-Einstein condensates (BECs) [7]. Among different nonlinear solutions there exists an interesting class of periodic solutions, the so-called breathers, which are periodic along the propagation and localized in the transverse direction. The importance of breathers that ride on a finite background has recently been recognized in the modeling of rogue waves [8,9]. Up to now these breathers have been categorized into two main types: longitudinal breathers and transverse breathers. The longitudinal breathers (generally referred to as Kuznetsov-Ma breathers (KMBs) [10, 11] oscillate longitudinally and are similar to the usual transversely localized breathing solutions of the NLS equation. The transverse breathers oscillate transversely and are localized in the propagation direction; one example is the Akhmediev breather (AB) [12]. When the periods of ABs and KMBs become infinite, they reduce to a fractional form that is called the rational solution – the Peregrine soliton [13].

The rogue wave is a special example of soliton solution with a non-zero background. At present, research on rogue waves has been extended to different systems [14–18] and significant progress has been achieved in both theoretical and experimental investigations in the past decade [19–21]. It is now accepted that KMBs and ABs are not rogue waves in the strict meaning of the word, but can be used in the modeling of ones. A true rogue wave – a giant solitary wave that is at least four times higher than the surrounding waves – can arise in the interactions of KMBs, ABs, and Peregrine solitons. This phenomenon is explicitly displayed in our analytical solutions. In addition, controllable rogue waves have also been extensively studied. For example, the management of rogue waves in inhomogeneous

#231582 - $15.00 USD Received 29 Dec 2014; revised 24 Jan 2015; accepted 26 Jan 2015; published 5 Feb 2015

nonlinear media was reported in [22–25]. In these papers only the dispersion (diffraction) and nonlinearity management were explored, which are usually considered as functions of the propagation distance [26–29]. However, this is not true in general anisotropic inhomogeneous nonlinear media. Actually, we have demonstrated that a more complete treatment should take into account the transverse inhomogeneity of optical media, which is commonly connected with the perturbation in the external potential [30]. This necessitates the inclusion of space-dependent coefficients in the appropriate evolution equation and the treatment by the similarity transformation method. It is worthwhile mentioning that the process of rogue wave generation needs to be controlled effectively, thus it is vital to understand theoretically how to realize such a control. Inspired by our previous work [30], we propose the ideas of transverse modulation and quantum modal parameter control, which are powerful tools for classifying and manipulating rogue waves.

In this paper, we theoretically investigate the behavior of rogue waves, based on the second-order breather solutions of the NLS equation with spatially-modulated coefficients and a special external potential. This research is realized by utilizing the NLS equation with a simple quadratic potential, modulated by the spatially-varying diffraction coefficient. The explicit solutions obtained are important for enabling a more easy understanding of rogue waves. The general solution contains two modulation frequencies (the complex eigenvalues) and the quantum modal parameter as variable parameters of the second-order breather, thus allowing one to choose a variety of particular cases with various patterns of such breathers. In Ref [31], Kedziora *et al.* used Taylor expansion method to study degenerate solutions. The difficulty of this method is the cumbersome calculation, involving mixed expansions in polynomials with trigonometric and hyperbolic functions. According to our method, one can obtain novel results more easily when the modulation frequencies are directly used.

The paper is organized as follows. In the next section we introduce the dimensionless nonlinear model with spatially modulated coefficients and a special external potential in the transversely-anisotropic inhomogeneous nonlinear media, and find the second-order breather solution for this model. In Sec. 3, we discuss different solutions by choosing two modulation frequencies and the quantum modal parameter appropriately; we present KMBs, ABs, and Peregrine solitons, and hybrid rogue wave solutions composed of those waves. Furthermore, the controllable behavior of these solutions is also investigated. In the last section, a conclusion is given.

## 2. Model and the second-order rogue wave solutions

We firstly recall results obtained in Refs [30, 31]. The NLS equation with spatially modulated coefficients and a special external potential can be written in the dimensionless form as [30]:

$$i\frac{\partial u}{\partial z}+\frac{1}{2}\beta(x)\frac{\partial^2 u}{\partial x^2}+\chi(x)|u|^2 u+\frac{1}{2}\beta(x)\left(-\frac{1}{4}x^2+m+\frac{1}{2}\right)u=0, \qquad (1)$$

where $u(z,x)$ represents the complex wave envelope, $z$ and $x$ are the dimensionless propagation distance and the transverse coordinate, $\beta(x)$ represents the diffraction coefficient, and $\chi(x)$ the nonlinearity coefficient. The non-negative integer $m$ is called the quantum modal parameter [30]. Here, the external potential is just a simple quadratic potential, modulated by the diffraction coefficient. In this way, we stay close to a common mathematical model of high physical relevance. For example, when $\beta$ is constant, one obtains the Gross-Pitaevskii equation with harmonic potential, which is of high importance in BECs [27, 30]. We proceed to search for the second-order breather solution of Eq. (1) and analyze how this solution is affected by the variation in the quantum modal parameter $m$. Equation (1) admits the following explicit solutions [30]:

#231582 - $15.00 USD Received 29 Dec 2014; revised 24 Jan 2015; accepted 26 Jan 2015; published 5 Feb 2015

$$u(z,x)=\sqrt{\frac{1}{\sqrt{2\pi}m!}}D_m(x)V(z,Y), \tag{2}$$

where $D_m(x)$ are the parabolic-cylinder functions. Following the similarity transformation method, the similarity variable $Y(x)$, the diffraction coefficient $\beta(x)$, and the nonlinearity coefficient $\chi(x)$ can be written as: $Y(x)=\sqrt{2\pi}m!\int dx/D_m^2(x)$, $\beta(x)=D_m^4(x)/2\pi(m!)^2$, and $\chi(x)=\sqrt{2\pi}m!/D_m^2(x)$. The complex field $V(z,Y)$ in Eq. (2), satisfies the standard NLS equation:

$$i\frac{\partial V}{\partial z}+\frac{1}{2}\frac{\partial^2 V}{\partial Y^2}+|V|^2V=0. \tag{3}$$

Equation (3) has been studied previously by many; of interest here are the solutions obtained by the Darboux transformation. Among other, Eq. (3) possesses the following second-order breather solution [31–33]

$$V(z,Y)=\left[1+\frac{G_2(z,Y)+iH_2(z,Y)}{D_2(z,Y)}\right]e^{iz}, \tag{4}$$

where $G_2$, $H_2$, and $D_2$ are given by

$$\begin{aligned}
G_2=&-\left(k_1^2-k_2^2\right)\left[\frac{k_1^2\delta_2}{k_2}\cos\mathrm{h}\left(\delta_1 z_{s1}\right)\cos\left(k_2Y_{s2}\right)-\left(k_1^2-k_2^2\right)\cos\mathrm{h}\left(\delta_1 z_{s1}\right)\cos\mathrm{h}\left(\delta_2 z_{s2}\right)\right.\\
&\left.-\frac{k_2^2\delta_1}{k_1}\cos\mathrm{h}\left(\delta_2 z_{s2}\right)\cos\left(k_1Y_{s1}\right)\right],\\
H_2=&-2\left(k_1^2-k_2^2\right)\delta_1\delta_2\left[\frac{1}{k_2}\sin\mathrm{h}\left(\delta_1 z_{s1}\right)\cos\left(k_2Y_{s2}\right)-\frac{1}{k_1}\sin\mathrm{h}\left(\delta_2 z_{s2}\right)\cos\left(k_1Y_{s1}\right)-\right.\\
&\left.\frac{1}{\delta_2}\sin\mathrm{h}\left(\delta_1 z_{s1}\right)\cos\mathrm{h}\left(\delta_2 z_{s2}\right)+\frac{1}{\delta_1}\sin\mathrm{h}\left(\delta_2 z_{s2}\right)\cos\mathrm{h}\left(\delta_1 z_{s1}\right)\right],\\
D_2=&\,2\left(k_1^2+k_2^2\right)\frac{\delta_1\delta_2}{k_1k_2}\cos\left(k_1Y_{s1}\right)\cos\left(k_2Y_{s2}\right)+\\
&4\delta_1\delta_2\left[\sin\left(k_1Y_{s1}\right)\sin\left(k_2Y_{s2}\right)+\sin\mathrm{h}\left(\delta_1 z_{s1}\right)\sin\mathrm{h}\left(\delta_2 z_{s2}\right)\right]-\\
&\left(2k_1^2-k_1^2k_2^2+2k_2^2\right)\cos\mathrm{h}\left(\delta_1 z_{s1}\right)\cos\mathrm{h}\left(\delta_2 z_{s2}\right)-\\
&2\left(k_1^2-k_2^2\right)\left[\frac{\delta_1}{k_1}\cos\left(k_1Y_{s1}\right)\cos\mathrm{h}\left(\delta_2 z_{s2}\right)-\frac{\delta_2}{k_2}\cos\left(k_2Y_{s2}\right)\cos\mathrm{h}\left(\delta_1 z_{s1}\right)\right].
\end{aligned}$$

The modulation frequencies $k_j=2\sqrt{1+\lambda_j^2}$ ($j=1,2$) are determined by the (complex) eigenvalues $\lambda_j$ that are independent of each other. In the above expressions, $z_{sj}=z-z_j$ and $Y_{sj}=Y-Y_j$ are the shifted variables from the point $(z_j,Y_j)$, and the instability growth rate of each component is $\delta_j=k_j\sqrt{4-k_j^2}/2$.

The modulation frequencies represent convenient parameters for classification of solutions, in addition to the quantum modal parameter *m*. For real modulation frequencies $k_j$,

#231582 - $15.00 USD Received 29 Dec 2014; revised 24 Jan 2015; accepted 26 Jan 2015; published 5 Feb 2015

as described in [31], solution (3) is capable of describing a variety of possible second-order breather profiles. Note that it must be $k_1 \neq k_2$, otherwise the solution (4) does not make sense, because then $V(z,Y)$ is trivial. The solution contains ABs, KMBs, the Peregrine soliton and their hybrids as particular solutions for different modulation frequencies and the modal parameter. For example, when two modulation frequencies are real, combinations of ABs and the Peregrine soliton are obtained – the breathers are extended along the $x$-direction; if the frequencies are a purely imaginary, the second-order breathers of different form develop along the $z$-direction. On the other hand, when one frequency is complex and the other one is purely imaginary, one obtains the nonlinear superposition of ABs and KMBs. Importantly, the emergence of true rogue waves, towering above the surrounding waves, is explicitly displayed in our analytical solutions. Thus, one is not compelled here to perform a statistical analysis of the resulting interfering breathers, to determine what percentage of those can be classified as true rogue waves. They are described analytically and appear at exactly prescribed positions.

## 3. Controllable behavior of second-order rogue waves

In this section, we discuss spatial distributions of solutions (2), developed in Section 2. We demonstrate that each case considered has its own distinct characteristics. The profiles of ABs, KMBs, and the Peregrine soliton appear similar even though the modulation frequencies take different values (*e.g.*, purely real or purely imaginary); the difference lies in the direction along which the intensities are distributed. It should also be mentioned that analytical solutions (2) and (4) explicitly depend on the similarity variable $Y(x)$ and the parabolic-cylinder function $D_m(x)$.

Our interest is in exploring effects of the two modulation frequencies $k_j$ in Eq. (2). According to Eq. (4), there exist four interesting families of the second-order breathers: the nonlinear superposition of two ABs, or an AB and a Peregrine soliton along the $x$-direction; the superposition of two KMBs, or of KMB and a Peregrine soliton along the $z$-direction; the superposition of Peregrine solitons; and the crossings of KMBs and ABs. Some of those cases will be displayed below. All these cases naturally depend on the values of two spatial frequencies $k_j$. Here, we will construct different types of the second-order rogue wave profiles depending also on the quantum modal parameter $m$. The influence of $m$ is to increase the spread and number of modes. The breather solutions of the standard NLS equation for purely real modulation frequencies $k_1$ and $k_2$ have been analyzed in Ref [31]. In the following, we discuss the cases where $k_j$ are purely imaginary or where they are complex.

In Fig. 1, we plot some examples of KMBs with the single fundamental second-order rogue wave in the middle, along the $z$-axis, and several KMBs with Peregrine solitons for two purely imaginary modulation frequencies, generated by solution (2) for different $m$. For small $m$, a typical example of such a KMB is shown in Fig. 1(a), which displays a periodic oscillation of the second-order rogue wave along the $z$-direction. Several single fundamental second-order rogue waves with "four-claw" symmetrical structures about the central peak [30] can be observed along the $x = 0$ line. Generally, there exist $m + 1$ KMBs, the intensity of which is zero at the center for odd $m$, while for even $m$ the maximum intensity is located at the center.

In addition, we present another special case in Fig. 1(b); the setup is as in Fig. 1(a) except for the beam shifts $x_1 = 1$ and $x_2 = -1$. Several KMBs mixed with Peregrine solitons are displayed in Fig. 1(b). When $m = 0$, a KMB and a Peregrine soliton are observed, as shown in the left panel of Fig. 1(b). When $m$ is increased to 1, two pairs of rogue waves are shown in the middle panel of Fig. 1(b). The intensity of the left pair is weaker than that of the right pair. For $m = 2$, there exist three pairs of beams in a more complex arrangement, see the right panel in Fig. 1(b).

According to our previous work [30], a second-order rogue wave can be built from three first-order rogue waves (three Peregrine solitons). Therefore, as long as suitable purely imaginary $k_1$ and $k_2$ are chosen (e.g. by decreasing $|k_1 - k_2|$), a new second-order breather

#231582 - $15.00 USD Received 29 Dec 2014; revised 24 Jan 2015; accepted 26 Jan 2015; published 5 Feb 2015

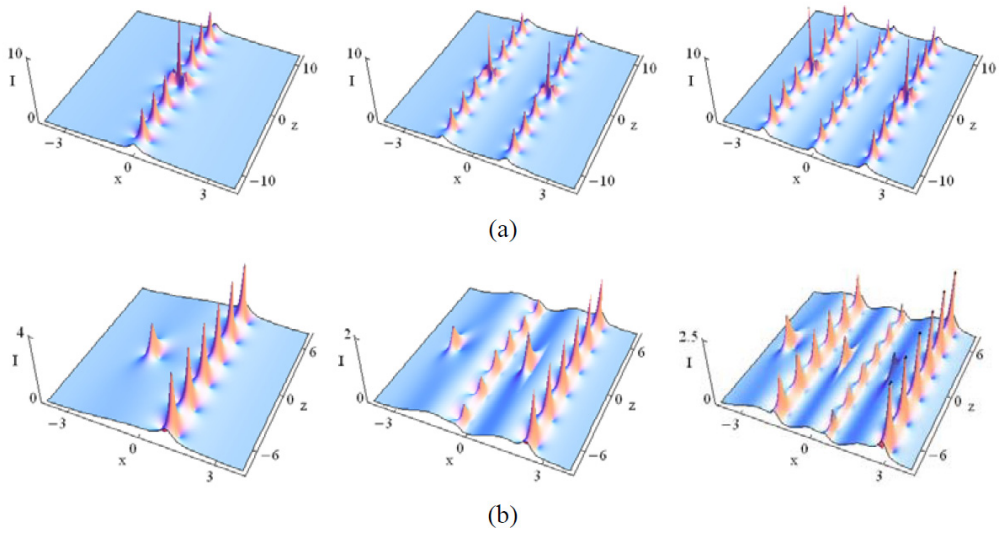


Fig. 1. Profiles of the second-order breathers, viewed as a nonlinear superposition of KMBs and Peregrine solitons. Here $k_1 = 1.7i$ and $k_2 = 0.3i$ for $m = 0,1,2$ from left to right. (a) Without transverse shifts. (b) With beam shifts $x_1 = 1$ and $x_2 = -1$.

family can be observed. Figure 2 exhibits some special profiles with $k_1 = 1.2i$ and $k_2 = 0.8i$. For $m = 0$, the distribution of a special second-order breather is depicted in the left panel of Fig. 2(a), in which there exist six Peregrine solitons that are equally distributed in $z<0$ and $z>0$ regions, respectively. One can see that the three Peregrine solitons form a triangle, and the one located at $x = 0$ is stronger than the other two. The phenomenon can be understood in the way that a second-order rogue wave located at $(z, x) = (-10, 0)$ splits into two second-order rogue waves during propagation, and then forms a second-order rogue wave with a large peak at $(z,x) = (0,0)$; this process proceeds inversely in the $z>0$ region, and finally a Peregrine soliton reappears at $(z,x) = (10,0)$. We speak of Peregrine solitons when the peaks are well isolated; strictly speaking this is not correct. In fact, the profile obtained represents a periodic oscillation of the second-order breather along the $z$-direction. If we choose $m = 1$, they form two pairs of breathers, see the right panel in Fig. 2(a). Note the formation of large rogue waves along the $x = 0$ line. Further increase in $m$ would lead to a repeated structure, formed similarly as in Fig. 1.

If the shifts along $x$-direction ($x_1 = 1$ and $x_2 = -1$) are considered, the results are shown in Fig. 2(b). For $m = 0$, the left panel in Fig. 2(b) displays two KMBs with different intensities and periods. There are three Peregrine solitons in the left row and six in the right row for the same propagation distance. When $m = 1$, similar results as in Fig. 1(b) are shown in the right panel of Fig. 2(b).

#231582 - $15.00 USD Received 29 Dec 2014; revised 24 Jan 2015; accepted 26 Jan 2015; published 5 Feb 2015

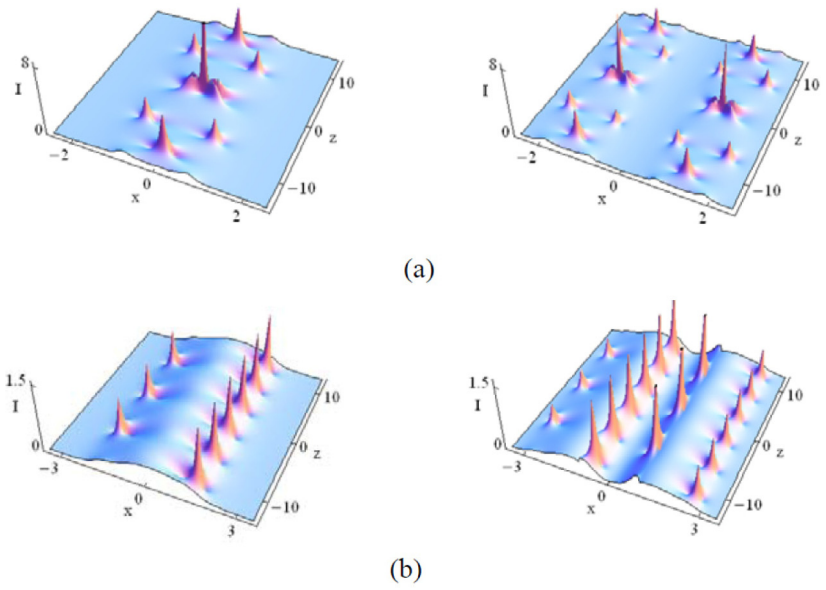


Fig. 2. Second-order breather solutions based on Peregrine solitons and KMBs. The setup and parameters are as in Fig. 1, except that $k_1 = 1.2i$ and $k_2 = 0.8i$. (a) Without transverse shifts. (b) With shifts $x_1 = 1$ and $x_2 = -1$.

Reducing further the value of $|k_1 - k_2|$ (we take now $k_1 = 1.3i$ and $k_2 = 1.4i$) leads to a different shape of the second-order breather, as shown in Fig. 3. In the left panel of Fig. 3(a), we depict the case with $m = 0$, in which three pairs of small Peregrine solitons along with a larger Peregrine soliton coexist around the single second-order rogue wave at the central position $(z,x) = (0,0)$. In comparison with Fig. 2(a), one can see that more small Peregrine solitons appear between the large Peregrine solitons in this oscillation process of the second-order rogue wave, due to the smaller value of $|k_1 - k_2|$. By increasing $m$ to 1, the structure from the left panel is doubled, as seen in the right panel of Fig. 3(a). From the analysis of Figs. 2 and 3, one can conclude that in the limit of $|k_1 - k_2| \to 0$, the second-order breather consisting of two rows of KMBs will appear (the crossing Peregrine solitons will disappear).

If we consider the shifts along $x$- and $z$-directions, we will obtain $m + 1$ pairs of KMBs, as exhibited in Fig. 3(b). Elucidated by these figures, we find that the periods of KMBs tend to be the same in the limit $|k_1 - k_2| \to 0$, which means that each pair of KMBs is exactly the same.

#231582 - $15.00 USD Received 29 Dec 2014; revised 24 Jan 2015; accepted 26 Jan 2015; published 5 Feb 2015

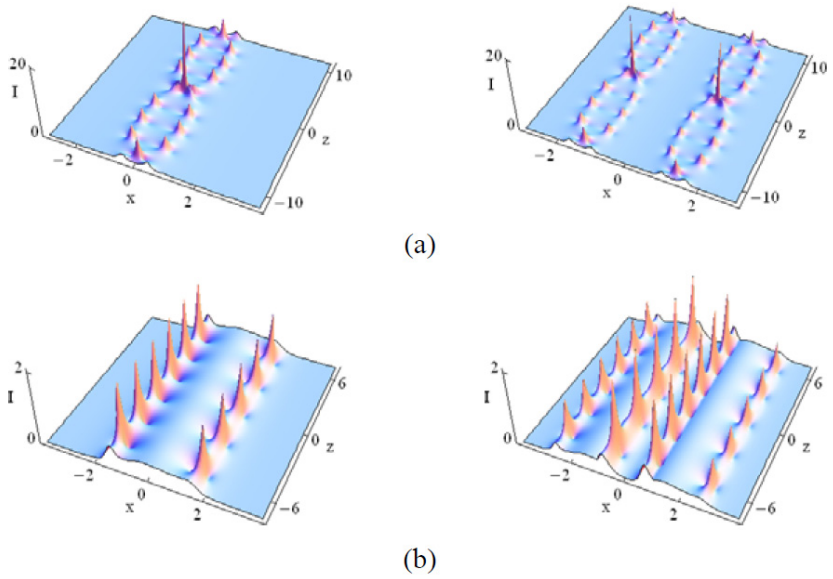


Fig. 3. Patterns of the second-order breathers with $k_1 = 1.3i$ and $k_2 = 1.4i$ for $m = 0,1$ from left to right. (a) Without shifts. (b) With shifts $x_1 = 1$, $x_2 = -1$, $z_1 = 5$ and $z_2 = -5$, respectively.

Finally, we investigate the second-order rogue wave solution with purely imaginary $k_1$ and a complex $k_2$. An interesting structure with several KMBs crossing an AB will form; the structures are plotted in Fig. 4. As a simple example, we choose $k_1 = 1.7i$ and $k_2 = 0.5 + 1.7i$. When one chooses $m = 0$, as shown in Fig. 4(a), the second-order breather is composed of an AB and a KMB. It is worth mentioning that the crossing point is a single fundamental second-order rogue wave with a "four-claw" symmetric structure around the central peak [30]. If we choose $m = 2$, the wave packet is formed by three KMBs and one AB, as displayed in Fig. 4(b). In general, these second-order breathers consist of $m + 1$ KMBs and one AB. The maximum intensity is at the central position when $m$ is even, but the intensity is zero there when $m$ is odd (not shown). Obviously, this is a typical nonlinear superposition of several KMBs crossing an AB.

For a more general case with two complex modulation frequencies $k_1 = a_1 + ib_1$ and $k_2 = a_2 + ib_2$, where $a_j \neq 0$ and $b_j \neq 0$, the profiles of the second-order breather are very complex, involving a number of crossing KMBs and ABs; a detailed analysis is beyond the interest of this paper, and might be an object of future exploration.

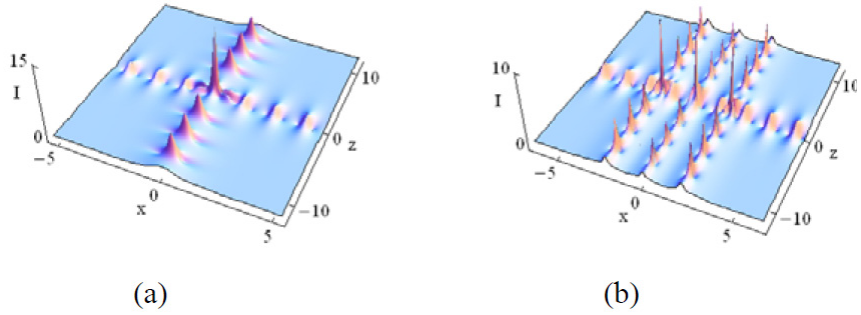


Fig. 4. KM breathers crossing an AB with $k_1 = 1.7i$ and $k_2 = 0.5 + 1.7i$ for $m = 0,2$ from left to right (without shifts).

#231582 - $15.00 USD Received 29 Dec 2014; revised 24 Jan 2015; accepted 26 Jan 2015; published 5 Feb 2015

## 4. Conclusion

In summary, we have investigated the NLS equation with a simple quadratic potential modulated by a spatial diffraction coefficient in an anisotropic inhomogeneous nonlinear medium. The second-order breather solutions are constructed by the similarity transformation. Different nonlinear superpositions of KMBs, ABs, and the Peregrine solitons are presented by selecting two modulation frequencies and the quantum modal parameter. The controllable behavior of KMBs, ABs, and Peregrine solitons forming second-order breather solutions is also discussed. An important message is that rogue waves can arise in the analytical second-order breather solutions of NLSE with a quadratic potential, without a need to invoke statistical methods to locate them. The results obtained here may be helpful in finding new ways of manipulating the second-order breathers experimentally in the inhomogeneous nonlinear media.

## Acknowledgments

This work was supported by the National Natural Science Foundation of China under grant No. 61275001 and by the Natural Science Foundation of Guangdong Province, China, under Grant No. 1414050004503. The work at the Texas A&M University at Qatar was supported by the NPRP 6-021-1-005 project with the Qatar National Research Fund (a member of the Qatar Foundation).

#231582 - $15.00 USD Received 29 Dec 2014; revised 24 Jan 2015; accepted 26 Jan 2015; published 5 Feb 2015